Biophysical Journal Volume 98 April 2010 1353–1363

The Photochemical Reaction Cycle and Photoinduced Proton Transfer of Sensory Rhodopsin II (Phoborhodopsin) from *Halobacterium salinarum*

Jun Tamogami,[†‡] Takashi Kikukawa,[†] Yoichi Ikeda,[‡] Ayaka Takemura,[‡] Makoto Demura,[†] and Naoki Kamo[†‡§*]
[†]Faculty of Advanced Life Science and [‡]Graduate School of Pharmaceutical Sciences, Hokkaido University, Sapporo, Japan; and [§]College of Pharmaceutical Sciences, Matsuyama University, Matsuyama, Ehime, Japan

ABSTRACT Sensory rhodopsin II (HsSRII, also called phoborhodopsin) is a negative phototaxis receptor of *Halobacterium salinarum*, a bacterium that avoids blue-green light. In this study, we expressed the protein in *Escherichia coli* cells, and reconstituted the purified protein with phosphatidylcholine. The reconstituted HsSRII was stable. We examined the photocycle by flash-photolysis spectroscopy in the time range of milliseconds to seconds, and measured proton uptake/release using a transparent indium-tin oxide electrode. The pKa of the counterion of the Schiff base, Asp^{73}, was 3.0. Below pH 3, the depleted band was observed on flash illumination, but the positive band in the difference spectra was not found. Above pH 3, the basic photocycle was HsSRII (490) → M (350) → O (520) → Y (490) → HsSRII, where the numbers in parentheses are the maximum wavelengths. The decay rate of O-intermediate and Y-intermediate were pH-independent, whereas the M-intermediate decay was pH-dependent. For $3 < pH < 4.5$, the M-decay was one phase, and the rate decreased with an increase in pH. For $4.5 < pH < 6.5$, the decay was one phase with pH-independent rates, and azide markedly accelerated the M-decay. These findings suggest the existence of a protonated amino acid residue (X-H) that may serve as a proton relay to reprotonate the Schiff base. Above pH 6.5, the M-decay showed two phases. The fast M-decay was pH-independent and originated from the molecule having a protonated X-H, and the slow M-decay originated from the molecule having a deprotonated X, in which the proton came directly from the outside. The analysis yielded a value of 7.5 for the pKa of X-H. The proton uptake and release occurred during M-decay and O-decay, respectively.

INTRODUCTION

Halobacteria have four retinal proteins: bacteriorhodopsin (BR) (1,2), halorhodopsin (HR) (3,4), sensory rhodopsin I (SRI) (5–7), and sensory rhodopsin II (SRII) (also called phoborhodopsin, pR) (8–11). Although these four have similar structures in which retinal as a chromophore binds to a specific lysine residue of the last of seven membrane helices (G-helix) (12), BR and HR function as light-driven ion pumps whereas SRI and SRII function as photoreceptors. On illumination, they undergo their own cyclic linear photochemical reactions (collectively called photocycle), which are similar to each other. The differences lie in the photocycling rates: ion-pumps have fast photocycles (~100 ms) whereas photoreceptors have slower cycles (~s). Another difference is that the sensory rhodopsins interact with transducer proteins. During the photocycle, the signal received by sensory rhodopsins is transmitted to the cytoplasm via the transducer protein. In response to this signal, halobacteria move toward the longer wavelength light (>520 nm, positive phototaxis) or avoid the shorter wavelength light (negative phototaxis) that includes harmful ultraviolet light. SRI (λ_{max} ~580 nm) is a receptor for positive phototaxis and its long-lived photointermediate (λ_{max} ~380 nm) is a receptor for negative phototaxis, while SRII (λ_{max} ~500 nm) is a receptor for negative phototaxis.

SRII was originally discovered in *Halobacterium salinarum* (formerly *halobium*) (8–11). There have been several studies on the photochemistry of this protein, but detailed research has proven difficult due to its low content, and due to its instability in the presence of detergent and under low salt conditions (13–15). It has been shown that *Natronomonas* (formerly *Natronobacterium*) *pharaonis* expresses a protein similar to sensory rhodopsin from *Halobacterium salinarum* (HsSRII) (pR) (16). This pigment was partially purified and named *pharaonis* phoborhodopsin (*p*pR, also called *N. pharaonis* SRII, NpSRII) (17), and its photochemistry was studied in greater detail because of its high stability (18–22). The subsequent success in expressing this opsin protein in *Escherichia coli* (23) further accelerated its biophysical investigation (24–28).

There have been several reports on the photochemical features of HsSRII using the membrane fragments (13–15, 29–31), and one of these studies reported that the photocycle contains K-, M-, N-, and O-intermediates (29). Sasaki and Spudich (30,31) reported that the proton circulates within the extracellular (EC) side, in contrast to transducer-free SRI and *p*pR (NpSRII), which transport protons from the cytoplasmic to the EC side on illumination (30–33). Nonetheless, the details of the proton circulation in HsSRII remain to be clarified. Thus, the proton movement and the detailed photocycle of HsSRII would be subjects of great interest, as would be the photosignaling transduction mechanism from HsSRII to its cognate transducer.

Submitted August 31, 2009, and accepted for publication December 9, 2009.
*Correspondence: nkamo@cc.matsuyama-u.ac.jp
Editor: Leonid S. Brown.

0006-3495/10/04/1353/11 $2.00
doi: 10.1016/j.bpj.2009.12.4288

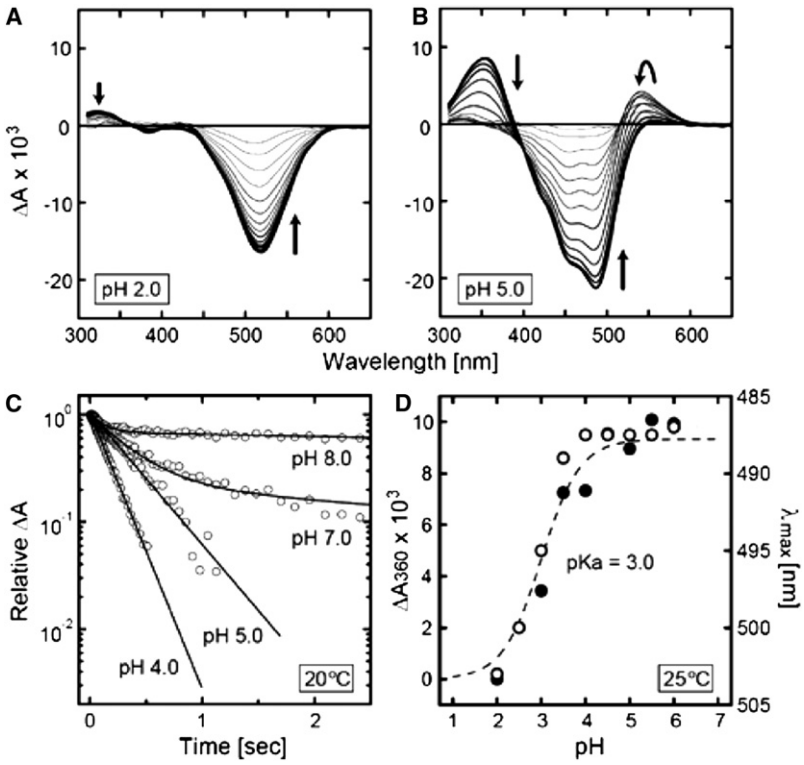

FIGURE 1 The flash-induced absorbance changes of HsSRII. (*A*) The flash-induced difference absorbance changes at pH 2.0 and (*B*) at pH 5.0. The bold line shows the difference spectrum at 10 ms after illumination. Traces of pH 2.0 are those at 10.1, 19.5, 37.1, 70.9, 135.1, 257.5, 490.9, and 935.3 ms, and at 1.78, 3.40, 6.47, 12.3, 23.5, 44.8, and 85.3 s after illumination. At pH 5.0, spectra from 10.1 ms to 44.8 s are depicted. (*C*) The semilogarithmic plot of the M-decay under varying pH. (*D*) The pH titration of λ_{max} shifts (*open circles*, *right ordinate*) and the M-yields (*solid circles*, *left ordinate*) are plotted against pH. The broken line is the curve simulated using the Henderson-Hasselbalch equation with a pKa of 3.0. Measurements were performed at 20°C (*A–C*) or 25°C (*D*) in solutions of 4 M NaCl and 10 mM six-mix buffer (citrate, MES, HEPES, MOPS, CHES, and CAPS) at the desired pH. The PC-reconstituted HsSRII (~10 μM) were encapsulated in 16.5% polyacrylamide gel.

The functional expression system of HsSRII in *E. coli* has been reported (34), and was shown to be essentially identical to the functional expression system for NpSRII (*p*pR) (23,35). The expression of various lengths of its cognate transducer in *E. coli* was also accomplished recently (36). In this study, we obtained HsSRII by the *E. coli* expression system. However, HsSRII solubilized with dodecyl-β-D-maltoside (DDM) was bleached by illumination in neutral and alkali solutions, which prevented the wide pH-range examination on photochemistry. In this article, we found that phospholipid-reconstituted samples were stable over wide pH (2 ~ 8) and temperature (10 ~ 40°C) ranges. Here, we investigated the photocycle of reconstituted HsSRII by flash-photolysis spectroscopy and the accompanying photo-induced proton uptake/release by the indium tin-oxide (ITO) method.

MATERIALS AND METHODS

Standard or reported methods were used. Detailed descriptions of the construction of expression plasmid (23,34), preparation of protein samples (34,37), flash-photolysis spectroscopy (38), ultraviolet-visible spectroscopy (39), and proton-transfer measurement using ITO (40,41) are given in the Supporting Material.

RESULTS

Photocycle overview

The photocycle of HsSRII was investigated by flash-photolysis spectroscopy on a millisecond timescale. Fig. 1 *A* (pH 2.0) shows the only negative band derived from depletion of the original HsSRII. In Fig. 1 *B* (pH 5.0), a positive band (λ_{max} ~360 nm) and a negative band (λ_{max} ~490 nm) with two shoulders (typically at 460 nm for the first shoulder and 420 nm for the second shoulder) appear immediately after the flash illumination. The former band is assigned to the M-intermediate (M). The latter is assigned to the depletion of the original HsSRII, because the spectrum with characteristic shoulders is very similar to that of the absorption spectrum of HsSRII in the dark (data not shown). As time passes, the positive band at ~540 nm rises with a concomitant decrease in M, and this intermediate is assigned as the O-intermediate (O). The λ_{max} of O of HsSRII is 525 nm whereas that of *p*pR (NpSRII) is 550 nm (20,42). The existence of these intermediates and their sequences are consistent with published results on HsSRII (15,29,36) or *p*pR (NpSRII) (20,42). Fig. 1 *C* shows the semilogarithmic plot of the M-decay under varying pH. Below pH ~6.5, M shows a one-phase decay, whereas above pH ~6.5, the M-decay shows two phases. As shown below, the pKa of the counterion of the Schiff base, Asp^{73}, is 3.0. Therefore, we should consider the photocycle in three pH regions: pH $<$ 3.0; 3.0 $<$ pH $<$ 6.5; and pH $>$ 6.5.

pKa of the counterion of the Schiff base, Asp^{73}

At pH 2.0 (Fig. 1 *A*), only the negative band was observed, and positive bands corresponding to M and O did not appear. The negative band is obviously the depletion of the original pigment whose λ_{max} is 520 nm, indicating a red shift of

~30 nm in acidic solutions. This shift is attributed to the protonation of the counterion of the protonated Schiff base, Asp^{73}, in the dark. Therefore, the λ_{max} values at various pHs are plotted with open circles in Fig. 1 *D*. On the other hand, the results in Fig. 1 *A* indicate that M did not form at pH 2.0. Obviously, this was due to the protonation of Asp^{73} in the dark. Therefore, the pH-dependent yields of flash-induced M may correlate with the pKa of Asp^{73}. The data represented by solid circles are the relative yields of flash-induced M, and are in good agreement with the λ_{max} shift. Analysis of these data yielded a pKa of 3.0 for Asp^{73} in the dark. This pKa value for L-α-phosphatidylcholine (PC)-reconstituted HsSRII is close to those determined previously (36,43), irrespective of the difference in lipids.

Photocycle at pH below the pKa of the counterion (pH 2.0)

Because M should not be produced because of the protonation of the counterion of the Schiff base, Asp^{73}, Fig. 1 *A* indicates the apparent absence of the O-like intermediate. On the other hand, Asp^{75} of *p*pR is the counterion of the Schiff base, and the photocycle of the D75N mutant of *p*pR has an O-like red-shifted intermediate (44). This suggests that an O-like intermediate also exists for the acid-form HsSRII. One assumes that the λ_{max} of this putative O-like intermediate would be very similar to that of the original pigment, and thus there would be no positive band. Note that the amount of the depletion of the original pigment is smaller than that at pH 5.0. (Compare the magnitudes of the negative bands in panels *A* and *B* of Fig. 1.) If the quantum yields of the acid and neutral forms of HsSRII are not largely different, this difference in the depletion might support this notion. In fact, the λ_{max} of the O-intermediate in the region of pH >3 is 520 nm, as shown below. The singular value decomposition analysis suggested the existence of two or three intermediates at pH 2, as shown in Fig. S1 in the Supporting Material. This might imply that one is an intermediate whose λ_{max} is close to the original pigment, and the other is Y-intermediate (Y), as described below. Another possibility is that the formation of the O-like intermediate is much faster than the present detection time-range. Further studies will be needed to resolve this matter.

Careful inspection of Fig. 1 *A* (pH 2.0) reveals the appearance of small positive band at shorter wavelength (below 350 nm). A similar band has also been observed in the wild-type *p*pR and V108M *p*pR mutant (45), but none of these bands has yet been identified.

Photocycle in the pH range of 3.0–6.5; existence of a Y- (or HsSRII′)-intermediate

As described above (Fig. 1 *C*), the M-decay in this pH range was one-exponential, and hence we assumed that the photocycle is the following sequential reaction scheme:

$$\text{HsSRII} \rightarrow \text{M} \xrightarrow{k_1} \text{O} \xrightarrow{k_2} \text{HsSRII}. \qquad \text{(Scheme A)}$$

Here, k_1 and k_2 are rate constants of M- and O-decay, respectively. There is a possibility that the conversion process of M to O may be reversible, but we neglected the reverse reaction. The obtained flash-photolysis data were analyzed with Scheme A. As shown in Fig. 1 *B*, the absorption maxima of the original pigment and of M and O in the difference spectra are 490, 360, and 540 nm, respectively. Hence, we monitored the absorbance changes at these three wavelengths. For the analysis, it was important to consider that each trace contains contributions from changes in the other components. The left column in Fig. 2 (analysis according to Scheme A) shows the comparison between the observed data and simulated curves. The fitting equations are described in the Supporting Material. The noisy lines represent the observed traces and the smooth lines are fitted curves. The thinner panels below the main panels depict the difference between the observed and regression curves at 490 nm. In the latter time region, when O decays or when its decay is complete (see the 540-nm traces), the differences in the thin panels become evident. A more detailed comparison under varying conditions (pH values of 3.5, 4.5, and 5.5; temperatures of 10°C, 25°C, and 40°C) is shown in Fig. S2. This led us to assume the existence of another intermediate denoted by Y after O, and the scheme was modified as follows:

$$\text{HsSRII} \rightarrow \text{M} \xrightarrow{k_1} \text{O} \xrightarrow{k_2} \text{Y} \xrightarrow{k_3} \text{HsSRII}. \qquad \text{(Scheme B)}$$

Here, k_3 is the rate constant of the Y-decay. The fitting equations are described in the Supporting Material. Some of the obtained results are shown in the right column of Fig. 2, where the observed and fitted curves coincide quite well. The good simulations of the experimental data under varying conditions are shown in Fig. S3. We also carried out a similar analysis using DDM-solubilized HsSRII in acidic pH (<6), and determined that Y is absolutely necessary for the complete fitting. (Note that at pH > 6, the pigment under DDM solubilization showed photobleaching.)

What is the intermediate Y? To answer this question, the spectrum of Y should be determined. As shown in Fig. 3 *B*, we determined the spectra of M, O, and Y from the flash-induced difference spectra shown in Fig. 3 *A* using the method described in the Supporting Material. The λ_{max} of Y is almost equal to that of HsSRII with a smaller extinction coefficient. In addition, this intermediate appears just before the original pigment. We therefore assume that the properties of Y are similar to those of the original pigment, which may also be assigned as HsSRII′. The bottom of the Y-spectrum is relatively wide, suggesting the contamination of O. If such contamination is present, we might consider the reverse change in the O-to-Y conversion. The Y-intermediate in this article may correspond to the P_7 or P_8 reported by Kim et al. (36). For *p*pR and HR, the corresponding

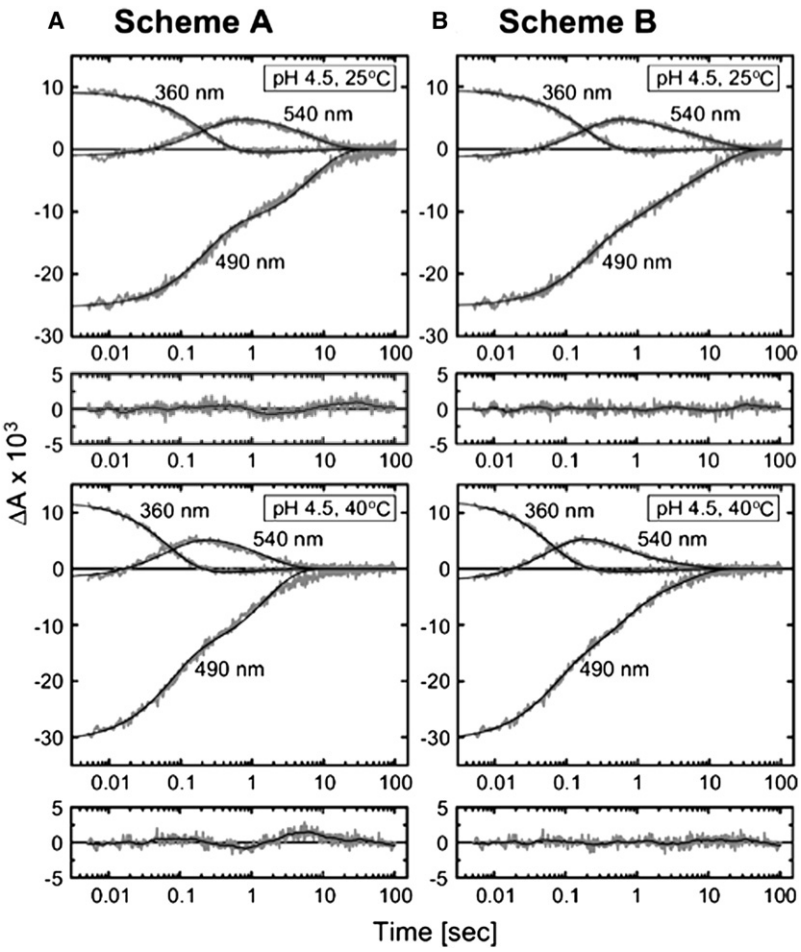

FIGURE 2 Photocycle Scheme B, but not photocycle Scheme A, successfully simulated the data. The panels in the left column were analyzed in accordance with Scheme A and those in the right column were analyzed in accordance with Scheme B. The noisy and smooth curves represent the observed and regression values. The thin panels indicate the difference between the observed and regression curves at 490 nm. The experimental conditions are the same as in Fig. 1.

intermediates (denoted by *p*pR′ and HR′) were also observed (46,47). Thus, the photocycle of HsSRII is written as

$$\mathrm{HsSRII} \rightarrow \mathrm{M} \overset{k_1}{\rightarrow} \mathrm{O} \overset{k_2}{\rightarrow} \mathrm{Y}\ (\mathrm{HsSRII}') \overset{k_3}{\rightarrow} \mathrm{HsSRII}. \quad \text{(Scheme C)}$$

In this study, we could not observe the N-intermediate. However, some previous works have proposed the presence of the N-intermediate (29,36). Furthermore, Kim et al. (36) proposed the existence of two M-intermediates. Future studies will be needed to try to detect these intermediates. However, we assume one M-intermediate in Scheme C.

Photocycle where pH > 6.5

In the medium with pH > 6.5, the decay of M shows two phases (Fig. 1 *C*). Some of the typical kinetic data shown in Fig. 4 reveal the biphasic decay of M (360-nm traces). More data obtained under varying conditions are shown in Fig. S4. The probable reasons for the two kinds of M-intermediates are as follows:

1. In the M-to-O conversion, the reverse reaction occurs.
2. The two different species of M decay through independent pathways.
3. The two different species of M decay sequentially but with slightly different absorption maximums.

From Fig. 4, especially from the data at pH 8.0, we can see that M (representing 360-nm absorbance) remained still after the complete disappearance of O (540 nm). This fact may rule out the possibility of reasons 1 and 3 if we take Scheme C as a basic photocycle. Therefore, we adopt the possibility of reason 2, and assume the following parallel two-reaction scheme:

$$\begin{aligned} &\text{Photocycle a: } \mathrm{HsSRII_a} \rightarrow \mathrm{M_a} \overset{k_{1a}}{\rightarrow} \mathrm{O_a} \overset{k_{2a}}{\rightarrow} \mathrm{Y_a} \overset{k_{3a}}{\rightarrow} \mathrm{HsSRII_a} \\ &\text{Photocycle b: } \mathrm{HsSRII_b} \rightarrow \mathrm{M_b} \overset{k_{1b}}{\rightarrow} (\mathrm{O_b}) \rightarrow (\mathrm{Y_b}) \rightarrow \mathrm{HsSRII_b} \end{aligned}. \quad \text{(Scheme D)}$$

Here, photocycles a and b occur independently. In Fig. 4, the fast decay of M matches the rise of O, whereas the second rise of O, which should match the slow decay of M_b, is missing. The reason may be that appreciable amounts of O_b are not produced due to the very slow decay of the M_b. Therefore, in the following analysis, O_b and Y_b are omitted. The flash-photolysis data should be analyzed according to the following scheme:

$$\Delta A = \alpha(\text{photocycle a}) + \beta(\text{photocycle b}). \quad \text{(Scheme E)}$$

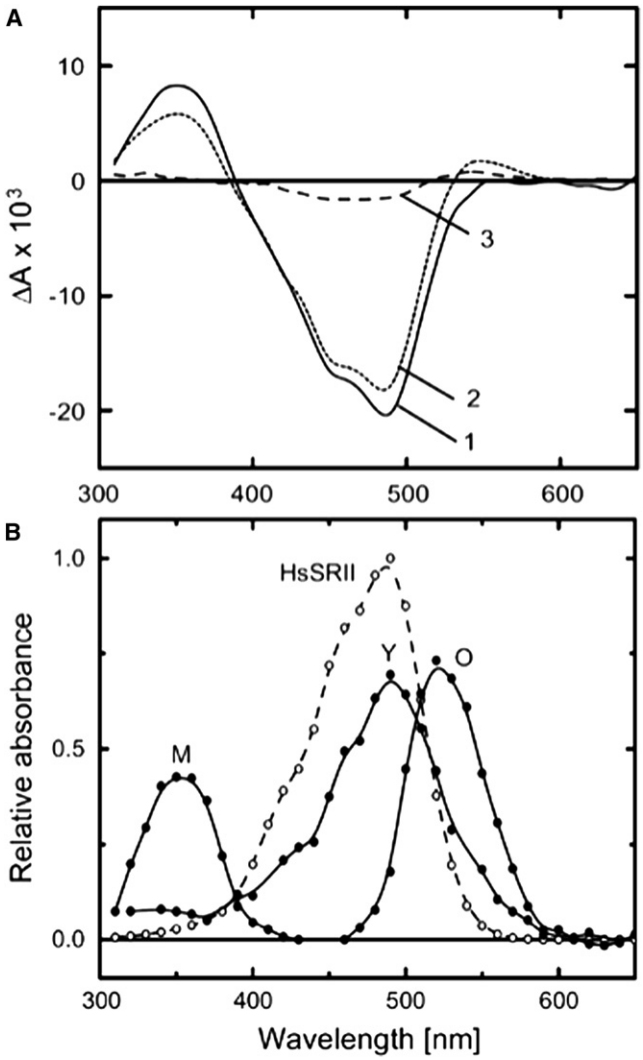

FIGURE 3 Estimated spectra of HsSRII and its intermediates of M, O, and Y. (*A*) Selected light-dark difference spectra for the calculation of M, O, and Y spectra. The spectra at 3.1 ms, 135.1 ms, and 23.5 s are selected, and denoted as curves 1, 2, and 3, respectively. (*B*) Estimated spectra of HsSRII, M, O, and Y. The broken line indicates the spectrum of HsSRII, and solid lines represent the spectra of the M-, O-, and Y-intermediates at pH 5.0 and 20°C.

The parameters to be determined are four kinetic parameters (k_{1a}, k_{2a}, k_{3a}, and k_{1b}), and α and β. We analyzed data obtained under various conditions (pH 6.0, 6.5, 7.0, 7.5, and 8; temperature 10°C, 20°C, 25°C, 30°C, and 40°C). Fitting was successfully achieved, and representative results are shown in Fig. S4. When we omitted Y, the agreement was poor (data not shown), suggesting the existence of this intermediate at this pH range. Values of

$$f_\alpha \left(= \frac{\alpha}{\alpha + \beta} \right)$$

and

$$f_\beta \left(= \frac{\beta}{\alpha + \beta} \right)$$

at 20°C are plotted in Fig. 5 using solid and open symbols, respectively. It can be seen that the molecules having a fast photocycle decrease with an increase of pH if the extinction coefficients of species do not depend on pH. The two curves cross each other, and analysis conducted using the Henderson-Hasselbalch equation yields a pKa of 7.3 ~ 7.8 (at 10–40°C). This fact may imply that a certain amino acid residue whose pKa is ~7.5 plays an important role; when this amino acid residue is protonated, the M-decay is fast (photocycle a), and when it is deprotonated, the M-decay is slow (photocycle b). The existence of an amino acid residue with a pKa of ~7.5 was pointed out previously (30).

Rate constants in the pH range from 3 to 8

The rate constants thus determined are plotted in Fig. 6. The temperature was 25°C. The rate constants of M-decay (k_1, k_{1a}, and k_{1b}) are plotted in Fig. 6 *A*, and the values of k_2 and k_3 are plotted in Fig. 6 *B*. The ordinate scales are the same for both. As is shown clearly, the M-decay rate constants (k_1, k_{1a}, or k_{1b}) are pH-dependent. Hence, the proton transfer is a rate-determining step for the M-decay. On the other hand, the O-decay rates are almost independent of pH but are associated with the proton transfer (see below), and the rates are temperature-dependent (see below). These facts may indicate that the rate-determining step of O-decay is a conformational change.

Thermodynamic analysis of the photocycle

Eyring plots of the rate constants were drawn, and the results at pH 3.0, 5.0, and 7.0 are shown in Fig. S5. These plots show the linear relationship of

$$\ln\left(\frac{k}{T}\right) = \ln\left(\frac{k_B}{h}\right) + \frac{\Delta S^\#}{R} - \frac{\Delta H^\#}{RT}.$$

Here, k_B, h, R, $\Delta S^\#$, and $\Delta H^\#$ are the Boltzmann constant, Planck constant, gas constant, activated entropy change, and activated enthalpy change, respectively. Estimated values of $\Delta S^\#$ and $\Delta H^\#$ are listed in Table S1. It is interesting that the $\Delta S^\#$ values for all conversions are negative, although some data seem to have errors. As shown in Fig. 6, the slowest step is the conversion from Y (HsSRII′) to HsSRII (where pH < 7), and it is notable that the large negative $\Delta S^\#$ values of this conversion give rise to the small rate constants. The molecular explanation for these large negative $\Delta S^\#$ values awaits further study.

Photoinduced proton uptake/release at pH < 3, where the counterion is protonated

We measured the photoinduced proton uptake/release from the PC-reconstituted HsSRII using an ITO transparent electrode system (see Fig. 7). Here, the upward and downward deflections signify proton release and uptake, respectively. Fig. 7, curve *a* of panel *A*, shows the flash-induced ITO

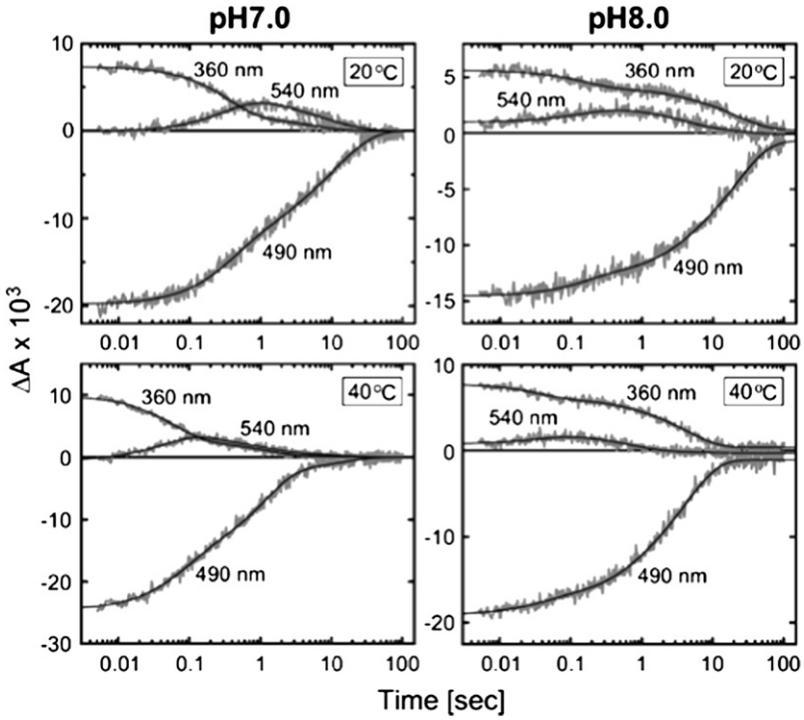

FIGURE 4 Under alkaline conditions the M-decay is biphasic. The smooth curves are fitted in accordance with Scheme D. The media were the same as those in Fig. 1.

signal at pH 2.0, where the counterion Asp^{73} is protonated. The proton release is observed first, followed by the uptake. This ITO signal suggests the existence of a photointermediate that decays with the time constant of ~0.20 s. The singular value decomposition analysis of the flash-photolysis data under the same conditions gave three time constants of 0.27, 5.7, and 47 s (data not shown), and the time constant of 0.27 may correspond roughly to that of ITO. It is noted that the time resolution of ITO is poor within this time-range (41). The λ_{max} of this intermediate might be close to that of the original HsSRII, as is considered above.

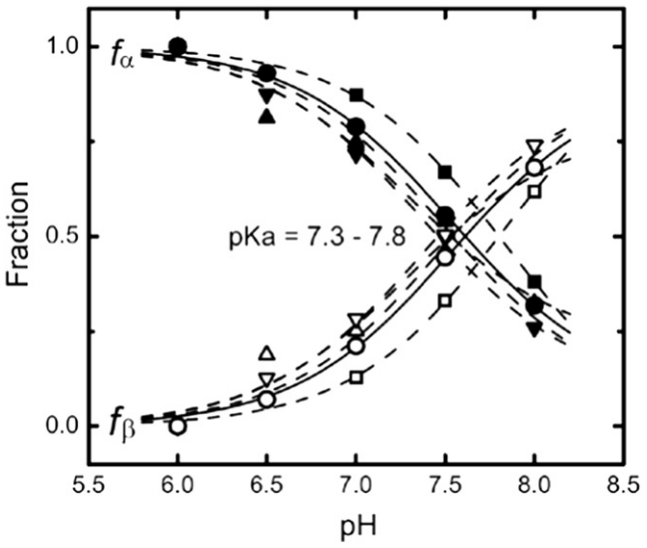

FIGURE 5 The pH-dependence of the amplitudes of photocycles a and b in Scheme D. The fractions of f_α (= $\alpha/(\alpha+\beta)$) and f_β (= $\beta/(\alpha+\beta)$) were plotted against pH. Solid symbols (■, ●, ▲, ▼) represent f_α at 10°C, 20°C, 25°C, and 40°C, respectively. Open symbols (□, ○, Δ, ∇) represent f_β at the same temperatures, respectively. The pKa values at 10°C, 20°C, 25°C, and 40°C were estimated as 7.8, 7.6, 7.3, and 7.5 by the Henderson-Hasselbalch equation.

Proton uptake/release in the pH range of 3.5–6.5

In Fig. 7 *A*, the ITO trace at pH 3.0 shows the first proton uptake followed by the proton release. As described above, the pKa of Asp^{73}, the counterion of the Schiff base, is estimated to be 3.0. Then, at this pH, approximately one-half of Asp^{73} is protonated, evoking the first proton release, whereas the other half is deprotonated, evoking the first proton uptake. The latter have larger effect, and thus the proton uptake may be observed first. At pH 5.0, the degree of uptake exceeds that at pH 3.0. The ITO-signal was compared with the flash-photolysis data (Fig. S6), and the M-decay was found to match well with the ITO signal. The correspondence between the two was further checked in the pH range from 3.5 to 6.0 (Fig. 7 *B*). As the pH increased, both the M-decay and ITO signals were delayed with good coincidence. These data reveal that proton uptake occurs during the decay of M (formation of O) in the pH range of 3.5–6.

The next question is when the proton release occurs. A plausible assumption is that proton release and dissociation of the protonated Asp^{73} occur during the O-decay. Unfortunately, a direct comparison between ITO and 540-nm signals may be meaningless, because the fidelity

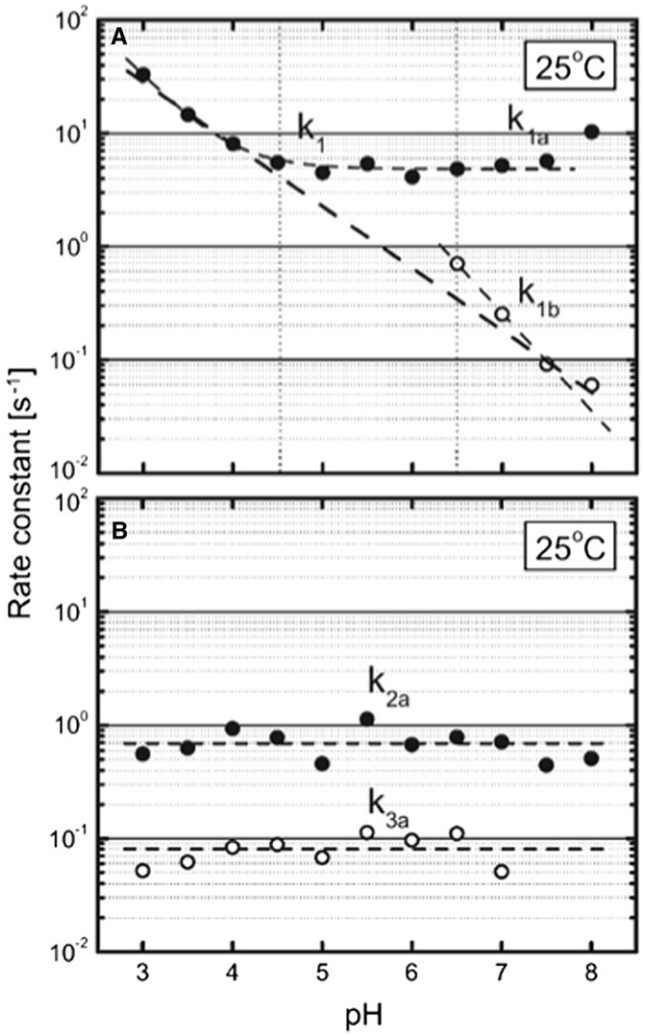

FIGURE 6 The pH-dependence of the decay-rate constants of photointermediates. (*A*) The plots of k_1 (k_{1a} (●) and k_{1b} (○)) against pH, and (*B*) the plots of k_{2a} (●) and k_{3a} (○) against pH at 25°C.

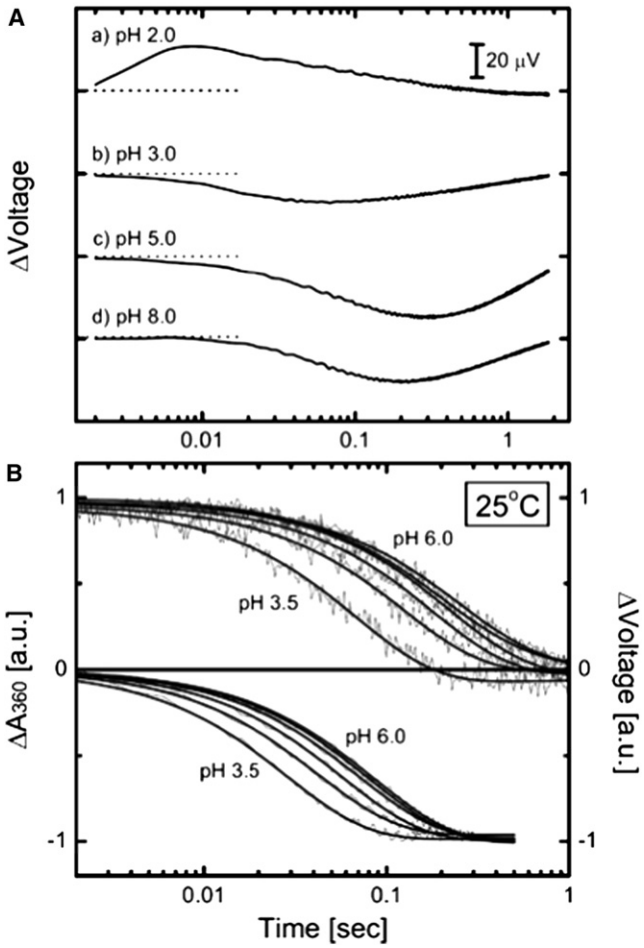

FIGURE 7 The flash-induced proton uptake/release measured with a transparent ITO electrode. (*A*) Traces obtained at (*a*) pH 2.0, (*b*) pH 3.0, (*c*) pH 5.0, and (*d*) pH 8.0 are shown. (*B*) Comparison of the time course between the flash-induced absorbance change and ITO signals under varying pH. (*Upper traces*) Flash-induced absorbance changes at 360 nm. (*Lower traces*) Flash-induced ITO signals at pH 3.5, 4.0, 4.5, 5.0, 5.5, and 6.0 in order of decreasing decay rates. The PC-reconstituted HsSRII samples (protein concentration of ~10–30 μM) deposited on an ITO electrode were used for measurements. The electric filter of the AC amplifier was set to a low cutoff of 0.08 Hz. For more detailed experimental conditions, see the Supporting Material.

of the time-dependent pH response of ITO becomes poor beginning at several hundred milliseconds after the flash (41). We therefore examined the OFF-response after the photo-steady state. After the photo-steady state by long illumination (~3 min), the response was recorded immediately after the light was removed. The results are shown in Fig. 8. At pH 3.5, the OFF-response is a proton-release. On the other hand, at pH 5 and 7, proton uptake occurs. Fig. 6 indicates that the slowest process at these three values of pH is the Y-decay, indicating that Y is the main component of the steady-state composition. Therefore, if proton release is associated with the Y-decay, we should observe proton release for all these pHs, but this was not the case in our results. When traces of pH 5 and 7 are compared, the extent of proton-uptake increases as pH increases. This may be interpreted as follows: As pH increases, the rate of M-decay becomes slow (see Figs. 1 and 6) so that the ratio of the M- to the O-intermediate at the steady state becomes large. Thus, the OFF-response is the proton uptake associated with M-decay. It is noteworthy that the signal overshoots the baseline, then returns to it, implying that proton-release occurs after M-decay. Azide is known as a reagent which accelerates the M-decay, which was also confirmed in our results (see below). In the presence of 200 mM azide, the OFF-response shows the first and short proton-uptake followed by proton release (Fig. 7 *A*, curve *d*), whereas the OFF-response in the absence of azide shows the proton uptake with small overshoot (Fig. 7 *A*, curve *c*). Although azide accelerates the M-decay, M may still be present. Therefore, the OFF-response shows the uptake first, but the magnitude is small compared with that of Fig. 7 *A*, curve *c*. Because azide accelerates the M-decay, the

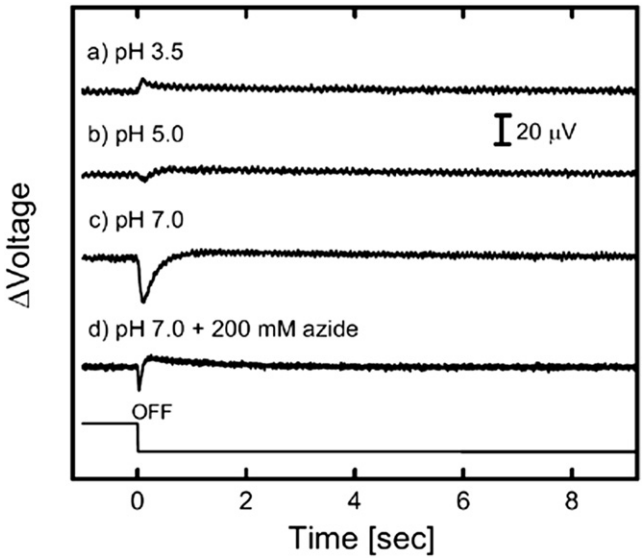

FIGURE 8 The OFF-response of the proton transfer after the photosteady state. The pH values are (*a*) pH 3.5, (*b*) pH 5.0, (*c*) pH 7.0, and (*d*) pH 7.0 in the presence of 200 mM azide. Upward and downward signals signify photoinduced proton release and uptake, respectively. Stationary light through an infrared filter (HA50 and IRA05) and a cutoff optical filter (Y44) was irradiated for ~3 min. The electric filter was set to a low cutoff of 5 Hz for measurements of stationary light-induced potential changes. The other experimental conditions were as described in Fig. 7.

subsequent O-decay starts immediately after the removal of light, and the proton release associated with the O-decay may become apparent. Thus, we may conclude that proton-uptake occurs during the M-decay, followed by release during the O-decay in which Asp^{73} dissociates.

Proton transfer in the region of pH > 6.5

In Fig. 7 *A*, the ITO trace at pH 8.0 is shown. As can be seen, the proton uptake is followed by release. Note that, at this pH, two photocycles occur. The rate shown in this figure is almost the same as that at pH 5.0, but its extent becomes small. Therefore, it is probable that this signal originates mainly from that of photocycle a in Scheme D, and that photocycle b is so slow that the proton transfer is not observable. However, it is feasible that proton uptake occurs during the M-decay of photocycle b, followed by proton release during the subsequent O-decay.

DISCUSSION

First, we discuss the photochemistry below pH 3—the range at which the counterion of protonated Schiff base is protonated. Although a photointermediate was not detected on a millisecond timescale (Fig. 1 *A*), such an intermediate may have been produced. Its spectrum could be similar to that of the original acid-form HsSRII, which would make detection impossible. The ITO signal of pH 2.0 shown in Fig. 7 supports this notion. A similar proton transfer is also observed for acid-form proteorhodopsin (PR) ((41) and J. Tamogami, T. Kikukawa, and N. Kamo, unpublished data). As M is not formed, this proton transfer may not associate with the deprotonation of the Schiff base. One possibility is that this proton transfer might occur through the transient deprotonation of $Asp^{198HsSRII}$ (corresponding to Asp^{212BR}), which is based on the assumption that the pKa of $Asp^{198HsSRII}$ is ~2.0, in contrast to Asp^{212BR}. In fact, one study has reported that the corresponding residue of *p*pR (NpSRII), Asp^{201pR}, has a pKa of 1.2 (48). However, the amino acid residues involved in the proton transfer and the direction of the proton movement were not clarified. Further studies will be needed to elucidate these points.

Fig. 6 *A* shows that there are three pH regions in relation to the M-decay rate: the region below pH 4.5, the region between 4.5 and 6.5, and the region above 6.5. When the pH is below 4.5, the M-decay rate is pH-dependent, implying that the proton comes directly from the bulk to the deprotonated Schiff base for M-decay. In the pH region between 4.5 and 6.5, the M-decay rate is pH-independent, implying that there is a certain protonated amino acid residue, denoted as X-H by Sasaki and Spudich (30,31). X-H serves as a proton donor, or as a relay for reprotonation of the Schiff base, as was pointed out previously (30,31). At the pH region above 6.5, two phases of M-decay were observed. In the faster photocycle (photocycle a), X-H may be involved. As the pH increases, the ratio of this cycle decreases, because X-H may dissociate in the unphotolyzed state (estimated pKa of ~7.5) and cannot serve as a proton donor or a proton-relay residue. When X-H is deprotonated completely, the proton in the bulk is used to reprotonate the Schiff base, which leads to the slower photocycle (photocycle b). The slope of k_{1b} against pH is almost unity (−0.86). Because of the low bulk proton, the rate is very slow.

What is the significance of the pH value of 4.5 (see Fig. 6)? According to the interpretation described above, below pH 4.5, X-H cannot dissociate in acidic media and does not serve as a proton donor or a proton-relay residue during the M-decay. Under the condition that X-H cannot function, the proton may come directly from the bulk to reprotonate the Schiff base. This may be a plausible mechanism. On the other hand, another assumption may be possible. In Fig. 6, interestingly, the k_1 values (pH < 4.5) are approximately continuous with those of k_{1b} (pH > 6.5), which is the rate constant of the direct proton entry from the bulk. The slope against pH in the pH region of 3–4.5 is smaller than unity, but the data seem to be concave. Therefore, one possibility is that two pathways are simultaneously active for the region of 3–6.5: the pathway via X-H and the direct entry of proton from the bulk.

Azide accelerates the M-decay of the D96N BR mutant that lacks the proton donor, whereas azide has no effect on the wild BR having the proton donor, Asp^{96BR} (49). Therefore, the acceleration of M-decay by addition of azide may offer a clue as to whether or not the proton-donor residue

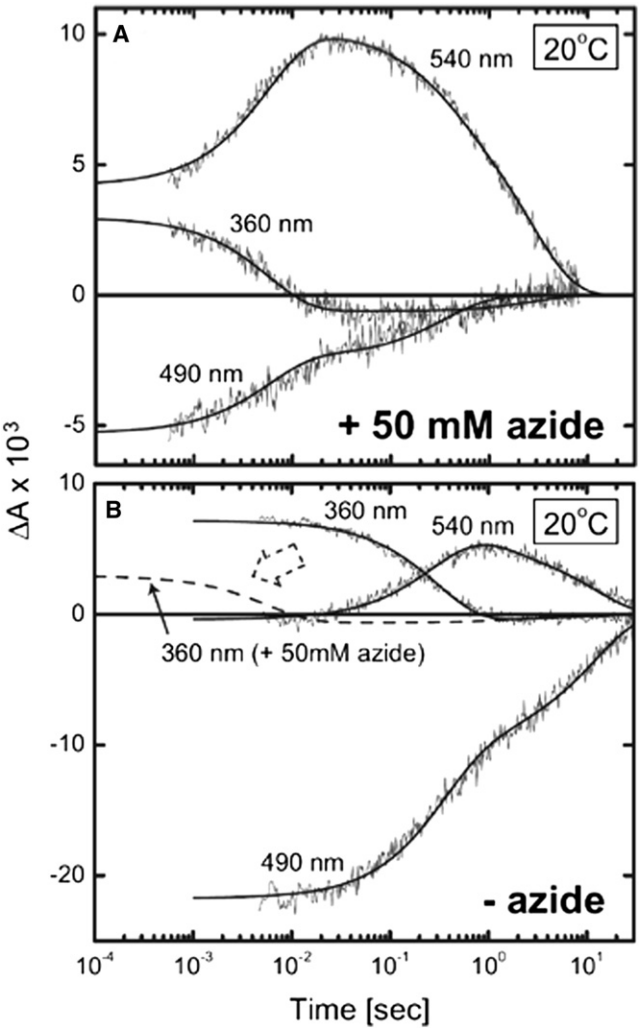

FIGURE 9 Azide is effective even though X-H functions. The flash-induced absorbance changes at 360, 490, and 540 nm in the presence (*A*) and absence (*B*) of 50 mM azide are shown. The noisy and smooth lines represent the observed and regression curves, respectively. The broken line in panel *B* represents the flash-induced absorbance changes at 360 nm (M-decay) in the presence of 50 mM azide, which shows 54-fold acceleration of M-decay in the absence of azide. Measurements were performed at pH 5.5 and 20°C.

exists. Fig. 9 shows the effect of azide (50 mM) on the M-decay of HsSRII at pH 5.5, where X-H may function, indicating the 54-fold acceleration of the M-decay. This may imply that X-H is not a residue that denotes a proton directly to the Schiff base, as is Asp^{96BR}, but a proton-relay residue. This also implies the existence of a pathway by which the proton enters directly from the bulk at pH 5.5 even though X-H obviously operates at this pH. From these results, we infer that, in all the pH regions ($3 < pH < 8.0$), the proton pathway ''from bulk'' is always available regardless of whether the pathway ''from X-H'' is available. These two pathways are denoted with their respective rate constants as

$$(\text{Pathway 1})\ \text{M} \xrightarrow{\text{from X–H}} \text{O}$$

(rate constant, $k_1^{(1)}$, which is pH-independent); and

$$(\text{Pathway 2})\ \text{M} \xrightarrow{\text{from bulk}} \text{O}$$

(rate constant, $k_1^{(2)}$, which is pH-dependent). Thus, the overall rate constant of M-decay should be $k_1^{(1)} + k_1^{(2)}$, and the pathway of 1 disappears when X-H dissociates completely. This report, to our knowledge, is the first to draw this conclusion.

Fig. 10 summarizes the conclusion of this investigation. The directions of the proton transfer of these two pathways are not known. Sasaki and Spudich (30) proposed the proton circulation in EC. For *p*pR (NpSRII) alone (without the transducer), the proton comes both from the extracellular and the intracellular space, and the intracellular path is closed for the complex of *p*pR (NpSRII) with the transducer (32,33). Hence, the M-decay kinetics of the HsSRII-transducer complex is very interesting, and warrants future investigation. In addition, the identification and the physiological role of the amino acid residue X-H should be clarified. Under physiological pH (pH 7 or 7.5), there are two kinds of HsSRII molecules (whose photocycles are a and b in Scheme D). This is not due to the reconstitution with PC, because Sasaki and Spudich (30) also found the two types of M using HsSRII in an *H. salinarum* membrane fraction. Which photocycle, then, evokes the phototaxis? Or are both active? These are subjects for future investigations.

SUPPORTING MATERIAL

Six figures and one table are available at http://www.biophysj.org/biophysj/supplemental/S0006-3495(09)06137-2.

REFERENCES

1. Haupts, U., J. Tittor, and D. Oesterhelt. 1999. Closing in on bacteriorhodopsin: progress in understanding the molecule. *Annu. Rev. Biophys. Biomol. Struct.* 28:367–399.
2. Lanyi, J. K. 2006. Proton transfers in the bacteriorhodopsin photocycle. *Biochim. Biophys. Acta.* 1757:1012–1018.
3. Váró, G. 2000. Analogies between halorhodopsin and bacteriorhodopsin. *Biochim. Biophys. Acta.* 1460:220–229.
4. Mukohata, Y., K. Ihara, …, Y. Sugiyama. 1999. Halobacterial rhodopsins. *J. Biochem.* 125:649–657.
5. Bogomolni, R. A., and J. L. Spudich. 1982. Identification of a third rhodopsin-like pigment in phototactic *Halobacterium halobium*. *Proc. Natl. Acad. Sci. USA.* 79:6250–6254.
6. Hazemoto, N., N. Kamo, …, M. Tsuda. 1983. Photochemistry of two rhodopsinlike pigments in bacteriorhodopsin-free mutant of *Halobacterium halobium*. *Biophys. J.* 44:59–64.
7. Spudich, J. L., and R. A. Bogomolni. 1984. Mechanism of color discrimination by a bacterial sensory rhodopsin. *Nature.* 312:509–513.
8. Takahashi, T., H. Tomioka, …, Y. Kobatake. 1985. A photosystem other than PS370 also mediates the negative phototaxis of *Halobacterium halobium*. *FEMS Microbiol. Lett.* 28:161–164.
9. Tomioka, H., T. Takahashi, …, Y. Kobatake. 1986. Flash spectrophotometric identification of a fourth rhodopsin-like pigment in *Halobacterium halobium*. *Biochem. Biophys. Res. Commun.* 139: 389–395.

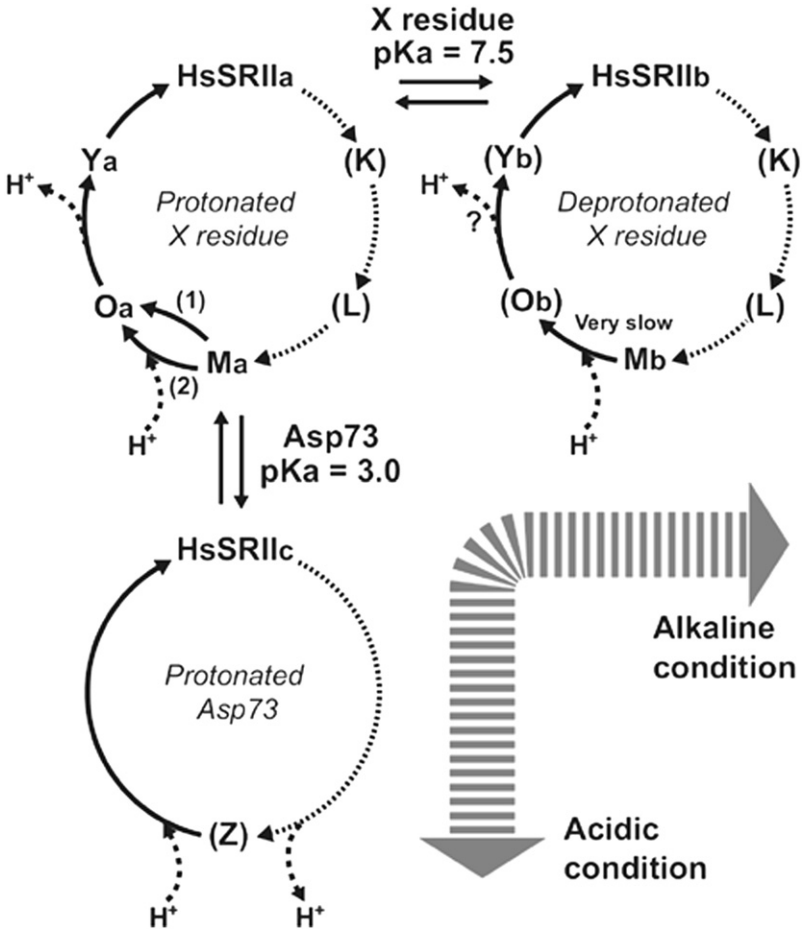

FIGURE 10 Our proposed pH-dependent photocycle of HsSRII. The photointermediate Z is hypothetical. When M_a decays, the deprotonated Schiff base becomes reprotonated through two pathways: one via X-H and one via the diffusion from the bulk. For M_b decay, the proton comes directly from the bulk to reprotonate the Schiff base.

10. Wolff, E. K., R. A. Bogomolni, …, W. Stoeckenius. 1986. Color discrimination in halobacteria: spectroscopic characterization of a second sensory receptor covering the blue-green region of the spectrum. *Proc. Natl. Acad. Sci. USA.* 83:7272–7276.
11. Spudich, E. N., S. A. Sundberg, …, J. L. Spudich. 1986. Properties of a second sensory receptor protein in *Halobacterium halobium* phototaxis. *Proteins.* 1:239–246.
12. Spudich, J. L., C. S. Yang, …, E. N. Spudich. 2000. Retinylidene proteins: structures and functions from archaea to humans. *Annu. Rev. Cell Dev. Biol.* 16:365–392.
13. Shichida, Y., Y. Imamoto, …, Y. Kobatake. 1988. Low-temperature spectrophotometry of phoborhodopsin. *FEBS Lett.* 236:333–336.
14. Imamoto, Y., Y. Shichida, …, Y. Kobatake. 1991. Photoreaction cycle of phoborhodopsin studied by low-temperature spectrophotometry. *Biochemistry.* 30:7416–7424.
15. Scharf, B., B. Pevec, …, M. Engelhard. 1992. Biochemical and photochemical properties of the photophobic receptors from *Halobacterium halobium* and *Natronobacterium pharaonis*. *Eur. J. Biochem.* 206:359–366.
16. Bivin, D. B., and W. Stoeckenius. 1986. Photoactive retinal pigments in haloalkaliphilic bacteria. *J. Gen. Microbiol.* 132:2167–2177.
17. Hirayama, J., Y. Imamoto, …, T. Yoshizawa. 1992. Photocycle of phoborhodopsin from haloalkaliphilic bacterium (*Natronobacterium pharaonis*) studied by low-temperature spectrophotometry. *Biochemistry.* 31:2093–2098.
18. Imamoto, Y., Y. Shichida, …, T. Yoshizawa. 1992. Chromophore configuration of *pharaonis* phoborhodopsin and its isomerization on photon absorption. *Biochemistry.* 31:2523–2528.
19. Imamoto, Y., Y. Shichida, …, T. Yoshizawa. 1992. Nanosecond laser photolysis of phoborhodopsin from *Natronobacterium pharaonis*: appearance of KL and L intermediates in the photocycle at room temperature. *Photochem. Photobiol.* 56:1129–1134.
20. Miyazaki, M., J. Hirayama, …, N. Kamo. 1992. Flash photolysis study on *pharaonis* phoborhodopsin from a haloalkaliphilic bacterium (*Natronobacterium pharaonis*). *Biochim. Biophys. Acta.* 1140:22–29.
21. Hirayama, J., Y. Imamoto, …, N. Kamo. 1994. Shape of the chromophore binding site in *pharaonis* phoborhodopsin from a study using retinal analogs. *Photochem. Photobiol.* 60:388–393.
22. Hirayma, J., N. Kamo, …, T. Yoshizawa. 1995. Reason for the lack of light-dark adaptation in *pharaonis* phoborhodopsin: reconstitution with 13-*cis*-retinal. *FEBS Lett.* 364:168–170.
23. Shimono, K., M. Iwamoto, …, N. Kamo. 1997. Functional expression of *pharaonis* phoborhodopsin in *Escherichia coli*. *FEBS Lett.* 420:54–56.
24. Kamo, N., K. Shimono, …, Y. Sudo. 2001. Photochemistry and photo-induced proton-transfer by *pharaonis* phoborhodopsin. *Biochemistry (Mosc.).* 66:1277–1282.
25. Spudich, J. L., and H. Luecke. 2002. Sensory rhodopsin II: functional insights from structure. *Curr. Opin. Struct. Biol.* 12:540–546.
26. Pebay-Peyroula, E., A. Royant, …, J. Navarro. 2002. Structural basis for sensory rhodopsin function. *Biochim. Biophys. Acta.* 1565:196–205.
27. Klare, J. P., and M. Engelhard. 2004. The archaeal sensory rhodopsin II/transducer complex: a model for transmembrane signal transfer. *FEBS Lett.* 564:219–224.
28. Moukhametzianov, R., J. P. Klare, …, V. I. Gordeliy. 2006. Development of the signal in sensory rhodopsin and its transfer to the cognate transducer. *Nature.* 440:115–119.
29. Sasaki, J., and J. L. Spudich. 1998. The transducer protein HtrII modulates the lifetimes of sensory rhodopsin II photointermediates. *Biophys. J.* 75:2435–2440.

30. Sasaki, J., and J. L. Spudich. 1999. Proton circulation during the photocycle of sensory rhodopsin II. *Biophys. J.* 77:2145–2152.

31. Sasaki, J., and J. L. Spudich. 2000. Proton transport by sensory rhodopsins and its modulation by transducer-binding. *Biochim. Biophys. Acta.* 1460:230–239.

32. Sudo, Y., M. Iwamoto, …, N. Kamo. 2001. Photo-induced proton transport of *pharaonis* phoborhodopsin (sensory rhodopsin II) is ceased by association with the transducer. *Biophys. J.* 80:916–922.

33. Schmies, G., M. Engelhard, …, E. Bamberg. 2001. Electrophysiological characterization of specific interactions between bacterial sensory rhodopsins and their transducers. *Proc. Natl. Acad. Sci. USA.* 98:1555–1559.

34. Mironova, O. S., R. G. Efremov, …, R. Schlesinger. 2005. Functional characterization of sensory rhodopsin II from *Halobacterium salinarum* expressed in *Escherichia coli*. *FEBS Lett.* 579:3147–3151.

35. Hohenfeld, I. P., A. A. Wegener, and M. Engelhard. 1999. Purification of histidine tagged bacteriorhodopsin, *pharaonis* halorhodopsin and *pharaonis* sensory rhodopsin II functionally expressed in *Escherichia coli*. *FEBS Lett.* 442:198–202.

36. Kim, Y.-J., I. Chizhov, and M. Engelhard. 2009. Functional expression of the signaling complex sensory rhodopsin II/transducer II from *Halobacterium salinarum* in *Escherichia coli*. *Photochem. Photobiol.* 85:521–528.

37. Scharf, B., B. Hess, and M. Engelhard. 1992. Chromophore of sensory rhodopsin II from *Halobacterium halobium*. *Biochemistry.* 31: 12486–12492.

38. Sato, M., T. Kikukawa, …, K. Nitta. 2003. Roles of Ser^{130} and Thr^{126} in chloride binding and photocycle of *pharaonis* halorhodopsin. *J. Biochem.* 134:151–158.

39. Chizhov, I., D. S. Chernavskii, …, B. Hess. 1996. Spectrally silent transitions in the bacteriorhodopsin photocycle. *Biophys. J.* 71:2329–2345.

40. Iwamoto, M., K. Shimono, …, N. Kamo. 1999. Light-induced proton uptake and release of *pharaonis* phoborhodopsin detected by a photoelectrochemical cell. *J. Phys. Chem. B.* 103:10311–10315.

41. Tamogami, J., T. Kikukawa, …, N. Kamo. 2009. A tin oxide transparent electrode provides the means for rapid time-resolved pH measurements: application to photoinduced proton transfer of bacteriorhodopsin and proteorhodopsin. *Photochem. Photobiol.* 85:578–589.

42. Chizhov, I., G. Schmies, …, M. Engelhard. 1998. The photophobic receptor from *Natronobacterium pharaonis*: temperature and pH dependencies of the photocycle of sensory rhodopsin II. *Biophys. J.* 75:999–1009.

43. Zhu, J., E. N. Spudich, …, J. L. Spudich. 1997. Effects of substitutions D73E, D73N, D103N and V106M on signaling and pH titration of sensory rhodopsin II. *Photochem. Photobiol.* 66:788–791.

44. Schmies, G., B. Lüttenberg, …, E. Bamberg. 2000. Sensory rhodopsin II from the haloalkaliphilic *Natronobacterium pharaonis*: light-activated proton transfer reactions. *Biophys. J.* 78:967–976.

45. Shimono, K., M. Iwamoto, …, N. Kamo. 1998. V108M mutant of *pharaonis* phoborhodopsin: substitution caused no absorption change but affected its M-state. *J. Biochem.* 124:404–409.

46. Váró, G., L. S. Brown, …, J. K. Lanyi. 1995. Light-driven chloride ion transport by halorhodopsin from *Natronobacterium pharaonis*. 1. The photochemical cycle. *Biochemistry.* 34:14490–14499.

47. Chizhov, I., and M. Engelhard. 2001. Temperature and halide dependence of the photocycle of halorhodopsin from *Natronobacterium pharaonis*. *Biophys. J.* 81:1600–1612.

48. Shimono, K., M. Kitami, …, N. Kamo. 2000. Involvement of two groups in reversal of the bathochromic shift of pharaonis phoborhodopsin by chloride at low pH. *Biophys. Chem.* 87:225–230.

49. Otto, H., T. Marti, …, M. P. Heyn. 1989. Aspartic acid-96 is the internal proton donor in the reprotonation of the Schiff base of bacteriorhodopsin. *Proc. Natl. Acad. Sci. USA.* 86:9228–9232.